Inorganic Chemistry

Article

pubs.acs.org/IC

Ligand-Field and Ligand-Binding Analysis of the Active Site of Copper-Bound Aβ Associated with Alzheimer's Disease

Chandradeep Ghosh and Somdatta Ghosh Dey*

Department of Inorganic Chemistry, Indian Association for the Cultivation of Science, Jadavpur, Kolkata, India 700032

Supporting Information

ABSTRACT: Alzheimer's disease (AD) patients show abnormally high concentrations of Cu^{2+} in the amyloid β plaques. This invokes that Cu^{2+} might play a crucial role in the onset of AD. The last few decades of research have also shown that Cu^{2+} plays a significant role in the aggregation of Aβ plaques in the brain and the generation of oxidative stress. Because the crystal structures of Cu-Aβ are yet to be obtained, there are various proposed models for the Cu^{2+} coordination environment of Aβ peptides. In this study, we have used the truncated hydrophilic part of the native Aβ peptide to probe the Cu^{2+} coordination site of the peptide, using a combination of spectroscopy and exogenous ligand-binding studies. It is evident from our study that Aβ(1−16) binds 1 equiv of Cu^{2+} and yet shows an equilibrium between two species with a pK_a of ∼8.1. Ligand-field analysis of absorption and circular dichroism spectroscopy data indicates five-coordinate geometry for both components. We investigate the effect of azide and 8-hydroxyquinoline binding to Cu-Aβ and demonstrate the presence of a water-derived ligand and a second exchangeable ligand coordinated to copper at physiological pH, along the equatorial plane of a square-pyramidal active site.

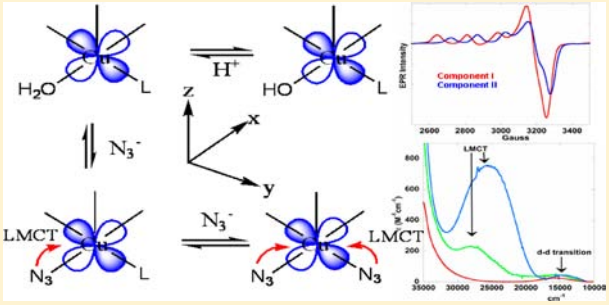

1. INTRODUCTION

Alzheimer's disease (AD) is the most common form of senile dementia. A total of 13% of people over the age of 65 years are affected by this terminal disease in the United States, and this number dramatically increases to 40% for people over the age of 85 years.[1] This fatal disease results from the deposition of amyloid β (Aβ) peptides in the brain.[2−4] The major symptoms of this disease are rapid mood swings, confusion, muscle immobility, long-term memory loss, and other age-related problems, finally leading to death.[5,6] Although Aβ is found to be neurotoxic at micromolar concentrations in vitro, it is produced in the brain at nanomolar concentrations[7] and possesses neurotrophic properties in cell culture.[8−10] Aβ, a small peptide containing 39 to 42 amino acid residues, is generated from a trans-membrane protein, known as amyloid precursor protein (APP).[11−14] β-Secretase cleaves APP at the Met671−Asp672 linkage to form the N terminus, while γ-secretase cleaves the protein at the Ala713−Thr714 linkage to generate the C terminus of Aβ(1−42).[15,16] Aβ peptides form plaques and oligomers in the neocortex region of the brain and affect the synapses between nerve cells, acting as a neurotoxic agent. The two most abundant isoforms of Aβ are Aβ(1−40) and Aβ(1−42). Aβ(1−40) is mainly found in biological fluids in soluble form,[17,18] whereas the latter is rather insoluble and is found in deposited senile plaques.[19] Autopsies of AD-affected brains have shown the presence of abnormally high levels of iron, copper, and zinc.[20−24] This indicates that these transition metals may have a significant role in the oligomerization or plaque formation of Aβ and the generation of oxidative stress associated with it. The last few years of research have also confirmed that these transition metals play a key role in the neurodegenerative process.[25−28]

Amyloidogenesis can be either accelerated or inhibited by Cu^{2+} depending on the condition and type of the aggregated state.[29] To understand the role of copper in AD, one needs to have a vivid idea about the interaction of Aβ with Cu^{2+}. Although there have been numerous studies on Cu-Aβ complexes over the last few decades, the crystal structures of Cu-Aβ complexes are yet to be solved. Different research groups have proposed structural models for Cu-Aβ complexes using different types of electron paramagnetic resonance (EPR) spectroscopy (CW, ESEEM, pulse ENDOR, and pulse HYSCORE), circular dichroism (CD), NMR, and X-ray absorption spectroscopy. However, many of the proposed models are controversial.

Initial studies suggest that Cu^{2+}-bound Aβ peptides have a 3N1O coordination environment.[30−38] The 3N coordination can be from either three histidine residues or two histidine residues and the N terminus (Scheme 1).[34,38−40] One of the nitrogen-donor atoms has also been proposed to be a deprotonated amide nitrogen.[41−43] The oxygen-binding residue can be Asp1, Asp7, Glu3, or Glu11, or it could be aqueous-buffer-derived.[37,44−46] The carbonyl oxygen atoms of the amide linkages are also possible copper-coordinating ligands.[47,48] Although there are reports of Tyr10 being the oxygen-donor ligand,[34,49] recent studies have ruled out this possibility.[40,44,50,51]

Received: August 27, 2012
Published: January 18, 2013

 © 2013 American Chemical Society dx.doi.org/10.1021/ic301865n | Inorg. Chem. 2013, 52, 1318−1327

Scheme 1. Some Representative Proposed Active Site Models of Cu-Aβ

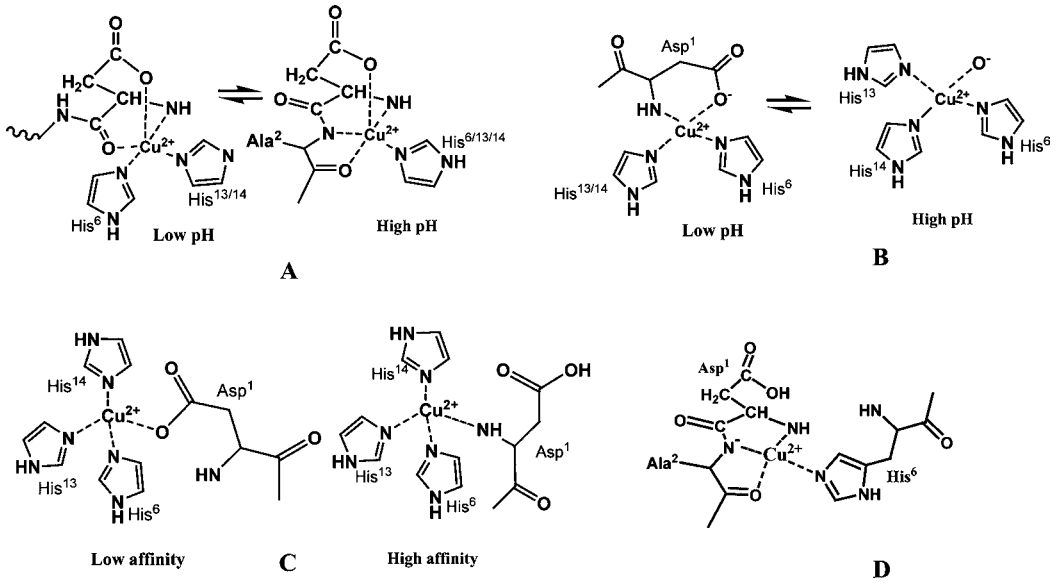

More recent studies indicate that Cu-Aβ complexes contain two different species, components I and II, which are in equilibrium in the range pH 5−9.[33,44,45,49,51−54] Different coordination environments have been proposed for these two components based on various spectroscopic data. A recent study on Aβ peptide containing N^{15}-labeled histidines reports that all three histidine residues simultaneously bind to Cu^{2+} at physiological pH.[55] A group of researchers have proposed two five-coordinate models for component I, having two histidine imidazoles (His6 and His13/His14), the N terminus, and the carboxylate group of Asp1 as the four Cu^{2+} binding ligands.[41−43] The fifth ligand was initially reported to be the peptide backbone carbonyl of the remaining histidine residue, based on ^{13}C and ^{1}H NMR,[42] which was later proposed to be the carbonyl group of the peptide bond in Asp1−Ala2 (Scheme 1A), based on CW, ESEEM, pulse ENDOR, and pulse HYSCORE EPR data.[41,43] The corresponding component II has been proposed to be coordinated to any one of the three histidines, the carbonyl group of the amide linkage of Ala2−Glu3, a deprotonated nitrogen atom of an amide bond, the N terminus, and the carboxylate group of Asp1.[41−43] HYSCORE data propose a four-coordinated Cu^{2+} environment for component I having two histidine imidazoles (His6 and His13/His14), the N terminus, and the carboxylate group of Asp1 as the coordinating ligands (Scheme 1B).[51] Component II has been proposed to be coordinated by three histidines along with the carboxylate group of Asp1. Another study based on HYSCORE spectroscopy on isotopically labeled peptides suggests binding of Cu^{2+} through the N terminus along with His6, His13, and the carbonyl oxygen of Asp1 in component I and three histidine ligands along with the carbonyl oxygen atom of the amide bond of Ala2−Glu3 in component II.[47] A recent computational study suggests coordination of the amide carbonyl of Ala2 along with the three histidine imidazoles as the Cu^{2+}-coordinating ligands.[48] There are also reports of three-histidine-bound models for both components I and II (namely, high and low affinity sites, respectively), where the fourth ligand is the carboxylate group of Asp1 for the high affinity site and the N terminus for the low affinity site (Scheme 1C).[44] Reports by Karr and Szalai indicate that $-COO^{-}$ of the Asp1 residue plays a key role as a hydrogen-bonding residue rather than directly taking part in Cu^{2+} coordination.[45] A recent report based on density functional theory (DFT) and molecular dynamics describes the N terminus, C═O(Asp1−Ala2), and two histidine imidazoles (His6 and His13 or His14) along with a water molecule as the five Cu^{2+}-binding ligands at low pH and the N terminus, N^{-}(Asp1−Ala2), C═O (Ala2−Glu3), His6, and a water molecule as the Cu^{2+}-coordinating ligands at high pH.[56] Most recently, another model for the Cu-Aβ active site has been proposed for the low-pH component I species, consisting of the N terminus, amidate nitrogen of the peptide bond of Asp1−Ala2, carbonyl oxygen of the amide bond of Ala2−Glu3, and one histidine imidazole (His6) using mass spectroscopy (Scheme 1D).[57]

Aβ(1−40) is the most abundant of the human Aβ peptides. The first 16 amino acids comprise the hydrophilic part, while the remaining 17−40 residues form the hydrophobic part of the peptide. Various studies based on EPR, Fourier transform infrared, X-ray absorption near-edge structure, etc., spectroscopic techniques have shown that metal binding to the hydrophilic Aβ(1−16) peptide fragment results in formation of the same active site as native Aβ(1−40) and is, hence, the choice of peptide for this study[36,40,50] (Figure S1 in the Supporting Information). In this study, we have used a combination of EPR, absorption, and CD spectroscopy on Cu^{2+}-Aβ(1−16) with the aim of understanding the coordination environment of Cu^{2+}-bound Aβ complexes. pH perturbation on the native Cu-Aβ complexes has been performed to elucidate the equilibrium of the two components present at physiological pH. Exogenous ligand binding can yield valuable insight into the electronic and geometric structures of the active site.[58−61] The effect of the addition of 8-hydroxyquinoline and azide as external ligands has been performed to detect the presence of labile ligands. Ligand-field analysis of the high and low pH data provides insight into the relative coordination environments of components I and II.

2. MATERIALS AND METHODS

All reagents were of the highest grade commercially available and were used without further purification. Amyloid β (Aβ) peptide 1−16 (sequence: Asp-Ala-Glu-Phe-Arg-His-Asp-Ser-Gly-Tyr-Glu-Val-His-His-Gln-Lys) and Asp1Asn mutant of Aβ(1−16) (sequence: Asn-Ala-Glu-Phe-Arg-His-Asp-Ser-Gly-Tyr-Glu-Val-His-His-Gln-Lys), used in

dx.doi.org/10.1021/ic301865n | Inorg. Chem. 2013, 52, 1318−1327

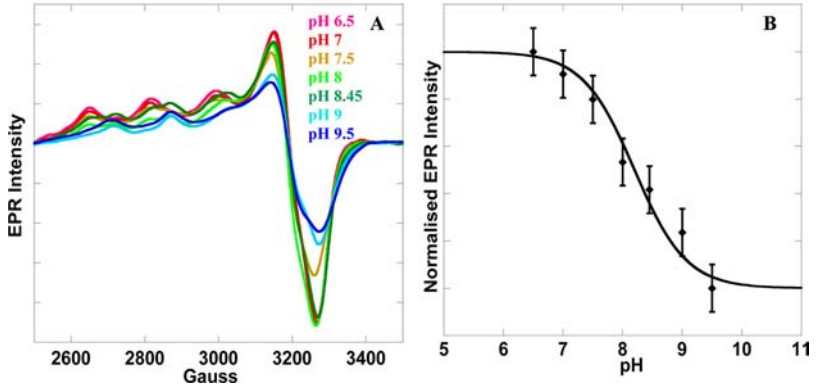

Figure 1. (A) EPR data of the Cu-Aβ complex at different pH values (pH 6.5 in MES, pH 7, 7.5, and 8 in HEPES, and pH 8.45, 9, and 9.5 in CHES). (B) pK_a plot.

this study were purchased from GL Biochem (Shanghai) Ltd. with >95% purity. Copper sulfate, sodium azide, and the buffers were purchased from Sigma. 8-Hydroxyquinoline was purchased from May and Baker Ltd. (England).

All of the pH 7−8 peptide stock solutions were made in 100 mM *N*-2-(hydroxyethyl)piperazine-*N*′-2-ethanesulfonic acid (HEPES) buffer. For the pH dependence study, the high-pH peptide solutions (pH 8.45−9.5) were made in 100 mM 2-(cyclohexylamino)ethylsulfonic acid (CHES) buffer and a low-pH peptide solution (pH 6.5) was prepared in 100 mM 2-(*N*-morpholino)ethanesulfonic acid (MES) buffer. The spectral features of Cu-Aβ were independent of the buffers used at a particular pH (Figure S2 in the Supporting Information). $CuSO_4$ was dissolved in nanopure water. All of the peptide stock solutions made for EPR measurements were 0.5 mM and 2 mM for absorption and CD measurements. The $CuSO_4$ stock solution was of 10 mM strength. Cu-Aβ complexes were prepared by incubating 1 equiv of an Aβ solution and 0.8 equiv of $CuSO_4$ solution for ∼1.5 h. For the concentration-dependent study, the equivalents of $CuSO_4$ were increased from 0.8 to 2.0 in the same peptide solution, and each time the sample was left to incubate for ∼1.5 h.

NaN_3 was dissolved in nanopure water to prepare 5 and 1 M stock solutions. Required volumes of a N_3^- solution were added to Cu-Aβ solutions prepared at different pH values to study the effect of azide. 8-Hydroxyquinoline was dissolved in nanopure water to prepare a 5 mM stock solution. A total of 1 equiv of a 8-hydroxyquinoline solution was added to a 0.5 mM solution of Cu-Aβ, prepared at different pH values. For the ligand-binding studies the equivalents of ligands added were calculated with respect to the Cu^{2+} concentration.

EPR spectra were obtained by a JEOL (JES FA200) spectrophotometer. EPR samples were 0.5 mM in concentration and were run at 77 K in a liquid-nitrogen finger Dewar. The EPR data have not been simulated. The *g* and *A* values have been extracted from the data.

Absorption spectral data were obtained by an UV−vis diode-array spectrophotometer (Agilent 8453), and CD spectra were obtained by a Jasco (J-815) CD spectrometer. The cuvettes used for UV and CD were made of quartz with 10 mm path length. The maximum absorbances obtained were in the range of 0.1−0.4 nm in the visible region of the spectrum for all absorption spectra. The ε values from the absorption data were obtained from different concentrations of the Cu-Aβ complexes in solution. The absorption and CD data were simultaneously fit using the program *PeakFit 4.0*. Gaussian analyses of the absorption and CD spectra were performed as follows: the same parameters (energy and bandwidth) were used to fit both the absorption and CD data in order to help constrain the fit. Minimum numbers of bands were used to adequately fit key features in both spectra.

The Cu^{2+} complex of the shorter peptide fragment, i.e., Aβ(1−16), has been denoted as Cu-Aβ, and that of the native peptide, i.e., Aβ(1−40), has been denoted as Cu-Aβ(1−40) in the text and figures.

3. RESULTS

3.1. Cu-Aβ at Low and High pH. *3.1.1. EPR Spectroscopy.* The EPR spectrum of 0.8 equiv of Cu^{2+}-incubated Aβ(1−16) at pH 7 recorded at 77 K shows an axial signal, with $g_z > g_{x,y} > 2.0$ indicating a $d_{x^2-y^2}$ ground state, having a set of hyperfine features corresponding to a major species and another set of weak hyperfine features corresponding to a minor species (Figure 1A, red). This is consistent with previous reports.[33,62] The predominant set of hyperfine features corresponds to component I, while the minor species reflect component II.[33] The intensities of the hyperfine features of components I and II are pH-sensitive.[33,53] With an increase in the pH, the intensity of component II starts to increase, while that of component I starts to decrease. Cu-Aβ shows an equilibrium between these two species in the range of pH 6.5−9.5 (Figure 1A) with a pK_a of ∼8.1 (Figure 1B). The EPR parameters of component I ($A_\parallel \sim 170$ and $g_\parallel \sim 2.239$) and component II ($A_\parallel \sim 159$ and $g_\parallel \sim 2.204$) differ significantly and are in agreement with previous reports.[33,53]

There are reports of a 2:1 stoichiometric ratio of Cu^{2+} to Aβ where one of the Cu^{2+} binding sites has been described as a high-affinity site and the other as a low-affinity site.[31,33,55] More recent studies reveal a 1:1 stoichiometric ratio of Cu^{2+} to Aβ in the Cu^{2+}-bound Aβ complex.[63,64] EPR spectra have been obtained by varying the Cu^{2+} concentration from 0.8 to 2.0 equiv relative to Aβ(1−16). When the Cu^{2+} concentration is increased from 0.8 to 1.2 equiv, the hyperfine features start to broaden (Figure 2). Increasing the Cu^{2+} concentration does not introduce any new

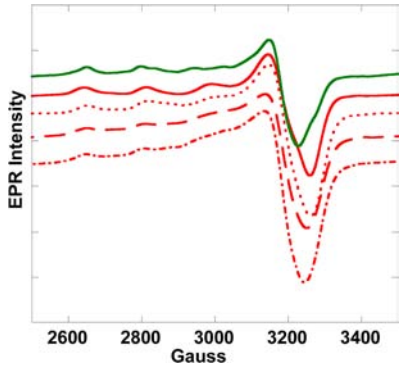

Figure 2. EPR spectra of Aβ(1−16) incubated with 0.8 (solid line), 1.2 (dotted line), 1.5 (dashed line), and 2.0 (dot-dashed line) equiv of Cu^{2+} and free $CuSO_4$ in a pH 7 HEPES buffer (green). The peptide concentration is 0.5 mM in a 100 mM HEPES buffer at pH 7.

dx.doi.org/10.1021/ic301865n | *Inorg. Chem.* 2013, 52, 1318−1327

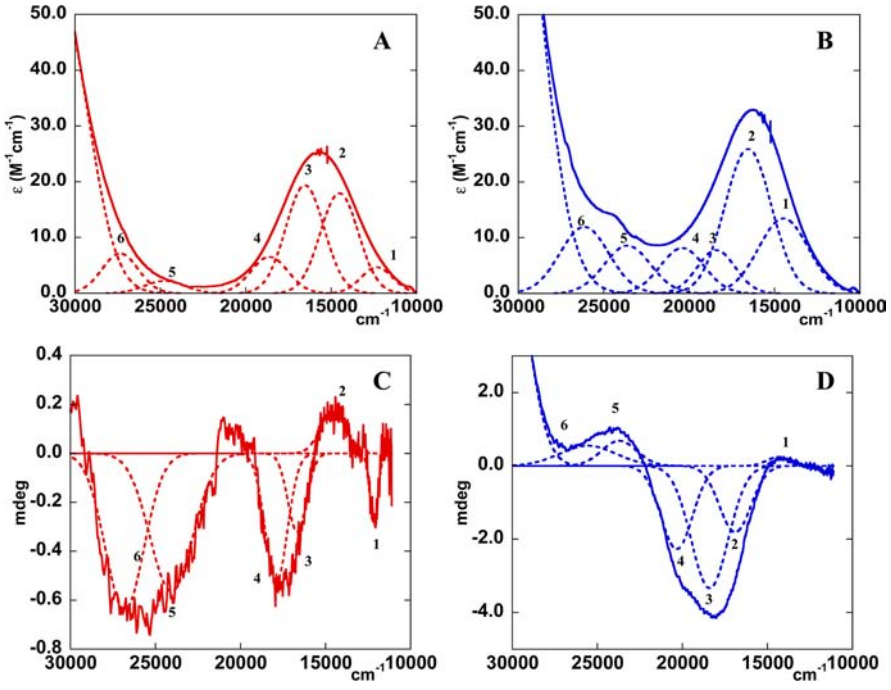

Figure 3. Room temperature optical data of Cu-Aβ: (A) pH 7 (in HEPES), absorption; (B) pH 9 (in CHES), absorption; (C) pH 7 (in HEPES), CD; (D) pH 9 (in CHES), CD.

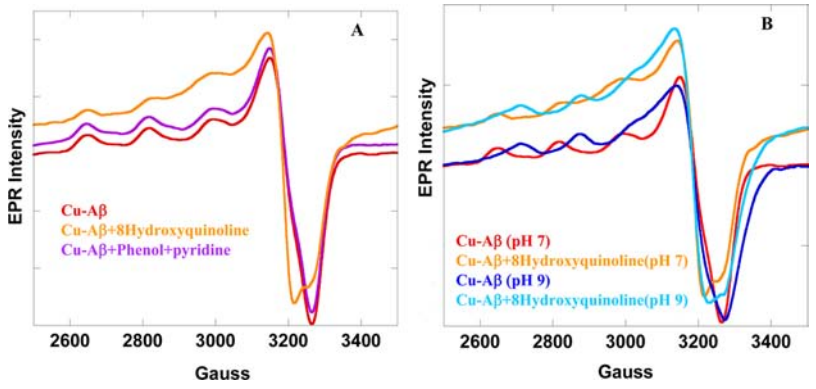

Figure 4. EPR spectra: (A) Cu-Aβ (red), Cu-Aβ and 1 equiv each of phenol and pyridine (purple), and Cu-Aβ and 1 equiv of 8-hydroxyquinoline (orange); (B) Cu-Aβ (pH 7; red), Cu-Aβ and 1 equiv of 8-hydroxyquinoline (pH 7; orange), Cu-Aβ (pH 9; blue), and Cu-Aβ and 1 equiv of 8-hydroxyquinoline (pH 9; light blue).

sets of hyperfine features corresponding to the minor component (i.e., component II) present at pH 7. Thus, components I and II of the Cu-Aβ complex originate from the same active site. The broadening of the spectrum upon the addition of excess Cu^{2+} could imply the presence of unbound Cu^{2+}. In fact, the difference spectrum of the EPR data of Cu-Aβ with 2.0 equiv of Cu^{2+} and 0.8 equiv of Cu^{2+} clearly indicates the presence of free copper (Figure S3 in the Supporting Information). Thus, the EPR experiments on the Cu-Aβ complexes prepared in our laboratory reproduce previously published results.[63,64]

3.1.2. Absorption and CD Spectroscopy. The absorption spectra of Cu-Aβ at both low and high pH are presented in Figures 3A,B and S4 in the Supporting Information. The spectra lack any intense charge-transfer (CT) bands in the visible region, which results in a colorless solution at room temperature. Overall, there is a blue shift of the ligand-field bands on going from low to high pH. The room temperature CD spectra of Cu-Aβ at both low and high pH are presented in Figures 3C,D and S4 in the Supporting Information, which also show a shift of ligand-field bands to higher energy with increasing pH, similar to the absorption data. A quantitative ligand-field description has been obtained from the simultaneous fit of the absorption and CD data (vide infra).

3.2. Effect of the Addition of Exogeneous Ligands at Low and High pH. Using the Cu-Aβ complex that reproduces the EPR parameters reported in the literature, the binding of monodentate and bidentate exogeneous ligands to the Cu-Aβ active site was explored.

3.2.1. 8-Hydroxyquinoline. 3.2.1.1. EPR Spectroscopy. When 1 equiv of 8-hydroxyquinoline is added to Cu-Aβ at pH 7, the EPR signal changes distinctly with enhanced rhombic character relative to the native Cu-Aβ spectrum (Figure 4A). This reflects that 8-hydroxyquinoline binds to Cu-Aβ. Because 8-hydroxyquinoline is a bidentate ligand, this invokes the presence of two weak adjacent exchangeable ligands bound to Cu-Aβ. Note that 8-hydroxyquinoline is analogous to clioquinol (5-chloro-7-iodo-8-quinolinol), which is a possible therapeutic agent for AD and is known for its metal-chelating properties.[65] Control experiments

dx.doi.org/10.1021/ic301865n | Inorg. Chem. 2013, 52, 1318−1327

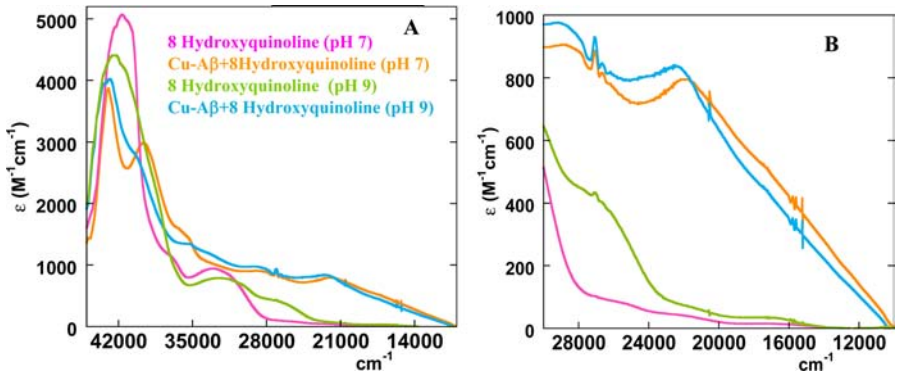

Figure 5. Absorption spectra of 8-hydroxyquinoline-bound Cu-Aβ at pH 7 (orange) and 9 (light blue) and free 8-hydroxyquinoline at pH 7 (pink) and 9 (green): (A) full spectra; (B) enlarged spectra.

by adding 1 equiv of phenol or pyridine or a mixture of phenol and pyridine (8-hydroxyquinoline contains both phenol and pyridine as the binding moieties) to Cu-Aβ produce very little effect on the EPR signal of Cu-Aβ (Figures 4A and S5 in the Supporting Information). This implies that, although weakly coordinating monodentate ligands cannot displace the ligands bound to Cu-Aβ, the chelating effect of 8-hydroxyquinoline can drive the displacement of the ligands.

When 8-hydroxyquinoline is added to Cu-Aβ at pH 9, similar significant spectral changes are observed relative to Cu-Aβ, implying binding of the bidentate ligand to component II (Figure 4B).

3.2.1.2. Absorption Spectroscopy. The absorption spectra of free 8-hydroxyquinoline and the ligand added to Cu-Aβ at pH 7 and 9 show distinct changes (Figure 5). This indicates that the ligand binds to both components I and II, as suggested by the EPR data (Figure 4B). Note that free $CuSO_4$ in the presence of excess 8-hydroxyquinoline shows no bands in the visible region of the spectrum, implying that the spectra obtained upon the addition of 8-hydroxyquinoline to Cu-Aβ is not due to the interaction of free Cu with the ligand (Figure S6 in the Supporting Information). There is a slight blue shift of the ligand-bound spectrum at high pH, relative to the low-pH data.

3.2.2. Azide. 3.2.2.1. EPR Spectroscopy. Cu-Aβ has been titrated with a solution of azide. The EPR data reflect two changes in the hyperfine features before yielding the final azide-bound-form spectrum (Figure 6). When this change in the hyperfine features was plotted against the azide concentration, it generated a biphasic plot (Figure S7 in the Supporting Information), implying 2 equiv of azide binding per 1 equiv of Cu-Aβ. This suggests the possibility of the presence of two weak exchangeable ligands bound to Cu-Aβ, consistent with the binding of bidentate 8-hydroxyquinoline (Figures 4 and 5). Analysis of the data generated binding constants of 0.01 and 0.001 for the 2 equiv of azide binding to Cu-Aβ. Note that the EPR spectrum of $CuSO_4$ in the presence of excess N_3^- clearly suggests that the complex formed after N_3^- addition to Cu-Aβ is very different from that of the free Cu^{2+} azide complex (Figure S8 in the Supporting Information).

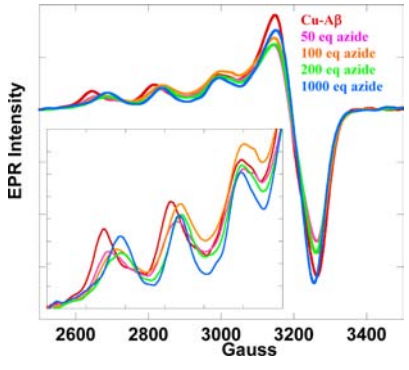

Figure 6. EPR spectra of (A) azide titration of Cu-Aβ at pH 7 (in HEPES).

The effect of azide binding to Cu-Aβ has been investigated at different pH values (Figure 7A). Although the hyperfine features of the azide-bound Cu-Aβ are significantly different from those of Cu-Aβ at lower pH (Figure S8 in the SI), where component I dominates, there is no effect of azide binding to Cu-Aβ at high pH, where component II dominates (Figure 7B). In other words, the high-pH spectrum of the azide-added Cu-Aβ solution resembles the high-pH component II species of Cu-Aβ. This suggests the presence of weak exchangeable ligands bound to Cu-Aβ at lower pH (component I). However, in component II, i.e., the high-pH form, the active site ligands cannot be displaced by azide.

3.2.2.1. Absorption Spectroscopy. The absorption spectrum upon azide addition to Cu-Aβ at pH 7 show two distinct bands upon the addition of ~200 equiv of azide relative to 1000 equiv of azide (Figure 8A). The intense bands in the spectrum indicate $N_3^- \rightarrow Cu^{2+}$ CT transitions.[66] A plot of the normalized absorbance at 540 nm against azide concentration generated a biphasic plot (Figure 8B, solid line), consistent with the EPR data. This implies that azide is sequentially displacing two ligands bound to copper, one of which has a weaker binding constant (displaced by ~200 equiv of azide) than the other (displaced by ~1000 equiv of azide). This supports the EPR data of azide addition (Figure 6) and 8-hydroxyquinoline addition to Cu-Aβ (Figures 4 and 5) at pH 7. When azide is added to Cu-Aβ at high pH, no intense bands were observed in the absorption spectrum, implying that azide is not binding to Cu-Aβ at high pH (Figure S9 in the Supporting Information). This is consistent with the EPR data of azide addition to Cu-Aβ at high pH (Figure 7B).

4. ANALYSIS

It is clear from the above results and existing literature that there are two different Cu-Aβ components at pH 7 (Figure 1A).[45,62] The EPR parameters ($A_{\|}$, $g_{\|}$, and $g_{\perp}$) of the wild-type peptide and Asp1Asn mutant (see below) are presented in Table 1. The EPR spectrum of Cu-Aβ at pH 7 in Figure 1 reveals that the proportion of component I is significantly higher relative to

dx.doi.org/10.1021/ic301865n | Inorg. Chem. 2013, 52, 1318−1327

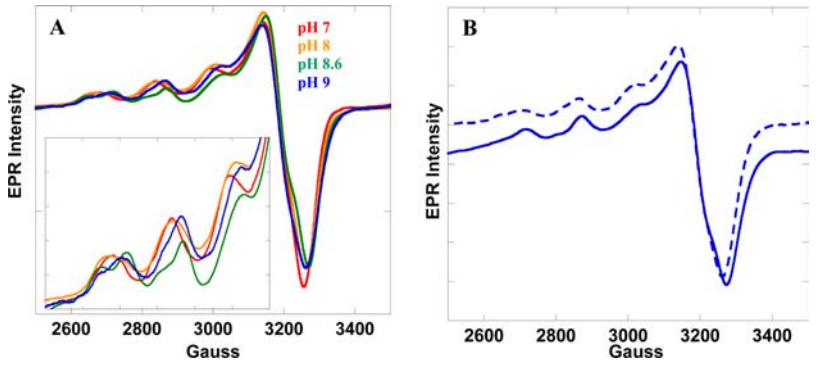

Figure 7. EPR spectra of (A) azide added to Cu-Aβ at different pH values. Inset: Enlarged low-field region of the EPR spectra (pH 7 and 8 in HEPES and pH 8.6 and 9 in CHES) and (B) Cu-Aβ (solid line) and Cu-Aβ + 1000 equiv of azide at pH 9 (dashed line; in CHES).

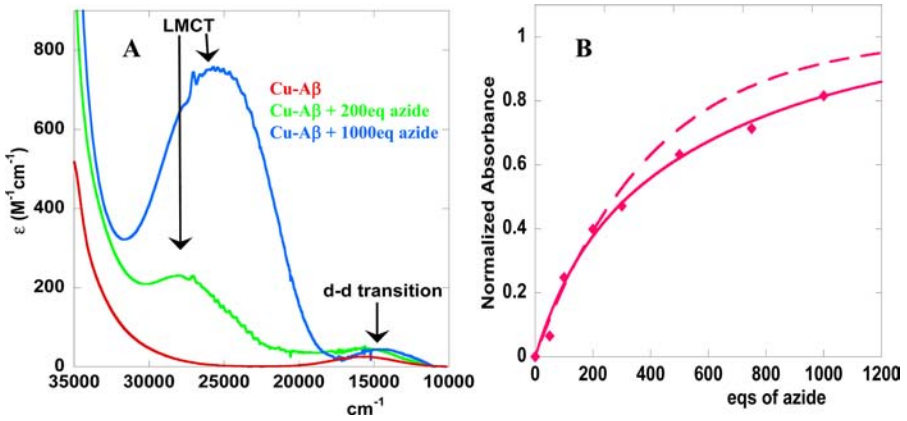

Figure 8. Absorption spectra upon the addition of 200 equiv (green) and 1000 equiv (light blue) of azide to Cu-Aβ compared with Cu-Aβ without azide (red) at pH 7. The LMCT and d → d transitions have been indicated. (B) Biphasic (solid line) and monophasic (dashed line) fits of changes in normalized absorbance at 540 nm as a function of the different concentrations of azide.

Table 1. $A_{\|}$, $g_{\|}$, $g_{\perp}$, and β^2 Values of Cu-Aβ(1 −16) and Cu-Aβ(Asp1Asn)

	component I				component II			
	$A_{\|}$	$g_{\|}$	$g_{\perp}$	β^2	$A_{\|}$	$g_{\|}$	$g_{\perp}$	β^2
Aβ(1−16)	170	2.239	2.046	0.68	159	2.204	2.042	0.61
Aβ(Asp1Asn)	171	2.237	2.046	0.68	154	2.203	2.045	0.61

component II. As reported by Karr and Szalai, the Asp1Asn mutant contains both components at physiological pH, however with a significantly higher ratio of component II to component I (Figure S10 in the Supporting Information).[45] To obtain the EPR spectrum of pure component I, a fraction of the spectrum of Cu-Aβ(Asp1Asn) was subtracted from that of Cu-Aβ. Similarly, to obtain the spectrum of pure component II, a fraction of this pure spectrum of component I of Cu-Aβ was subtracted from that of Cu-Aβ(Asp1Asn) (Figure 9). The subtractions were done such that no residual features of component II were present, as judged by the intensities of the hyperfine features, while obtaining the spectrum of pure component I and vice versa. Note that component II shows significant rhombic character.

The addition of pure spectra of components I and II (Figure 9) at a 1:1 ratio generates Figure 10A (purple). This generated spectrum is very similar to the experimentally obtained spectrum of Cu-Aβ at pH 8 (the pK_a of Cu-Aβ is 8.1 ± 0.1; Figure 10A). This implies that component II is actually the high-pH form of component I and components I and II are in pH equilibrium, agreeing with previous reports.[33,53] This has been further verified by overlaying the generated spectrum of component II with the

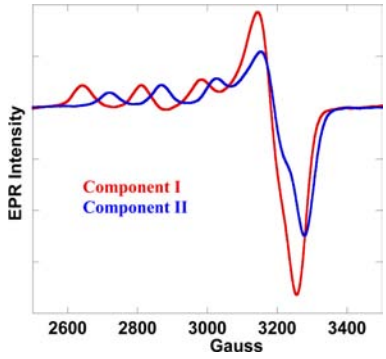

Figure 9. Generated spectra of pure component I and component II of Cu-Aβ.

spectrum of the high-pH form of Cu-Aβ (Figure 10B), which shows that they are identical. Additionally, when 2 equiv of Cu^{2+} is added to Aβ (Figure 10C, dotted red line), neither the component I nor component II EPR signal gets enhanced but rather the spectrum broadens. This implies that components I and II do not represent two different active sites, in which case

dx.doi.org/10.1021/ic301865n | Inorg. Chem. 2013, 52, 1318−1327

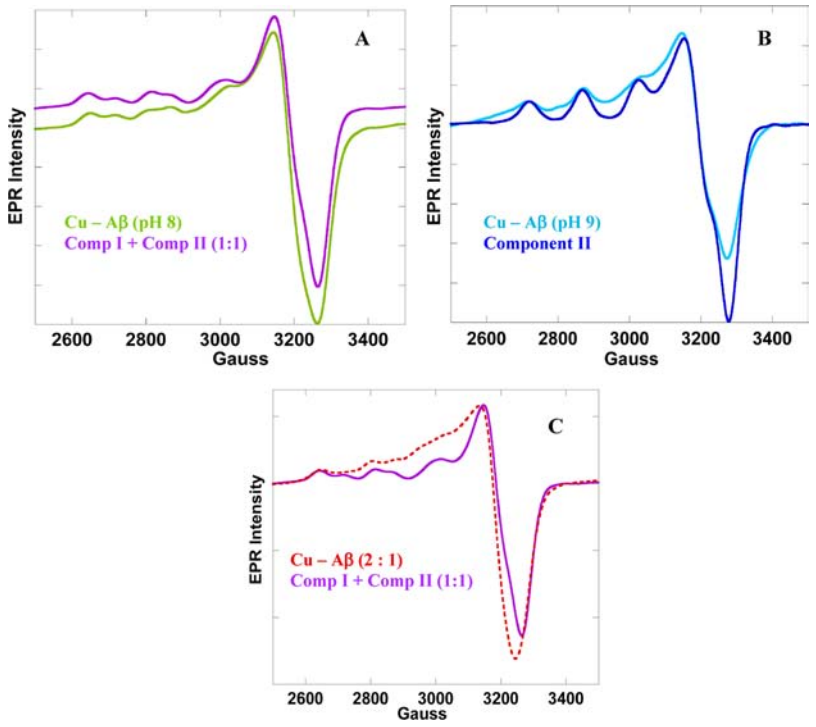

Figure 10. Comparison of the generated spectrum of (A) component I + component II in a 1:1 ratio (purple) with the experimentally obtained spectrum of Cu-Aβ at pH 8 (green), (B) component II (blue) with the experimentally obtained spectrum of Cu-Aβ at pH 9 (cyan), and (C) component I + component II in a 1:1 ratio (purple) with the spectrum experimentally obtained by adding 2 equiv of Cu^{2+} to 1 equiv of Aβ(1−16) (dashed red line).

the addition of the second 1 equiv of Cu^{2+} would have led to complete population of components I and II and their EPR hyperfine intensities would have increased relative to 1 equiv of copper.

Both the g_{II} and A_{II} values of component I are higher than those of component II. This can be analyzed to estimate the covalency of these sites. From ligand-field theory (LFT), the metal hyperfine coupling is given by the equation[67]

$$A_{\parallel} = Pd\left[-\kappa\beta^2 - \frac{4}{7}\beta^2 + (g_{\parallel} - 2.0023) + \frac{3}{7}(g_{\perp} - 2.0023)\right]$$

where $Pd[Cu^{2+}] = 400 \times 10^{-4}$ cm^{-1}, $\kappa[Cu^{2+}] = 0.43$, and $g_{\perp} = (g_x + g_y)/2$. This results in a calculated $\beta^2 = 0.68$ for component I and 0.61 for component II (β^2 reflects the covalency, i.e., the percentage Cu 3d character in the singly occupied molecular orbital; Table 2) for the Cu-Aβ complex. This means that

Table 2. $A_{\parallel}$, $g_{\parallel}$, $g_{\perp}$, and β^2 Values of Cu-Aβ-Bound Azide

	$A_{\parallel}$	$g_{\parallel}$	$g_{\perp}$	β^2	binding constant
Cu-Aβ + 200 equiv of azide	163	2.107	2.043	0.53	0.01
Cu-Aβ + 1000 equiv od azide	158	2.116	2.041	0.52	0.001

component I has ∼68% spin density on the copper and component II has only ∼61% of the spin density on copper. This significant decrease in the spin density on copper, which means a subsequent increase in the spin density on the ligands with an increase in the pH, can be explained by the presence of a more covalent ligand bound to copper at high pH. This is consistent with the presence of a protonation equilibrium between components I and II; i.e., component II has a deprotonated ligand, which is more covalent and, hence, causes delocalization of more spin density than a neutral ligand, present in component I.[68,69]

The absorption and CD data of Cu-Aβ at low and high pH (Figure 3) reflect a blue shift of the ligand-field bands with an increase in the pH (Table 3). This is consistent with the presence

Table 3. Transition Energies (cm^{-1}) of Ligand-Field (d → d) and CT Bands Obtained by the Simultaneous Fit of the Absorption and CD Data of Cu-Aβ at pH 7 (Component I) and 9 (Component II)

	transition energies (cm^{-1})		
band	pH 7	pH 9	assignment
1	12241	14417	d → d
2	14548	16720	d → d
3	16604	18404	d → d
4	18256	20368	d → d
5	24406	23661	CT
6	27087	25847	CT

of a deprotonated ligand to Cu-Aβ at high pH, which is a stronger ligand than the corresponding neutral ligand, bound at physiological pH.[70] The ligand-field transition energies (Table 3) are quite high for both components I and II for these Cu-Aβ complexes to be a four-coordinate site. Rather, the energies suggest that these are both five-coordinate.[71]

LFT predicts $g_{\parallel} = 2.0023 - 8\lambda\alpha^2\beta^2/(E_{xy} - E_{x^2-y^2})$, where λ for $Cu^{2+} = -830$ cm^{-1} and α is the metal coefficient in the d_{xy} orbital. Assuming that α^2 remains the same between components I and II and the wave function of d_{xy} does not change because it is nonbonding, the relative shifts of the $g_{\parallel}$ values can be used to

dx.doi.org/10.1021/ic301865n | Inorg. Chem. 2013, 52, 1318−1327

estimate the relative $d_{xy} \rightarrow d_{x^2-y^2}$ (ΔE) transition energies. The relative $\Delta E_I/\Delta E_{II} = \alpha_I^2/\alpha_{II}^2(0.92)$. Thus, assuming that α_I^2 and α_{II}^2 are not very different (d_{xy} is generally nonbonding in copper complexes with axial ligand field and assuming that the coordination geometry of the active site has not been dramatically perturbed between components I and II), the $d_{xy} \rightarrow d_{x^2-y^2}$ (ΔE) ligand-field transition of the lower-pH component I should shift to lower energy by a factor of ~0.9 relative to the corresponding transition of the high-pH component II. Although the $d_{xy} \rightarrow d_{x^2-y^2}$ transition cannot be assigned definitively from the absorption and CD data alone, simultaneous fits of the absorption and CD data indicate an average shift of all of the ligand-field transitions by ~2000 cm^{-1} (Figures 3 and S4 in the Supporting Information and Table 3). Thus, the low-pH ligand-field transitions are lower by a factor of 0.88−0.90 (Table 3) relative to the high-pH transitions, which is in good agreement with the ligand-field analysis of the EPR data.

Binding of azide to Cu-Aβ dramatically lowers β^2 from 0.68 in the resting form to 0.53 (Table 2) in the monoazide-bound form. This is suggestive of the formation of a covalent Cu−N_3^- bond, which is also supported by the observation of ligand-to-metal charge transfer (LMCT) bands in the absorption spectrum (Figure 8A). The remarkable decrease in β^2 is consistent with the replacement of a neutral ligand with an anionic N_3^- ligand at physiological pH. The replacement of the second ligand with N_3^- only marginally changes the β^2 value (Table 2).

The change in β^2 between the low and high pH forms suggests that the ligand involved in the pH equilibrium is in the equatorial plane. This will allow its overlap with the $d_{x^2-y^2}$ orbital containing the unpaired electron (the $d_{x^2-y^2}$ ground state is implied by the axial EPR spectrum). Also, the additional lone pair on the deprotonated ligand (component II), which is not involved in σ bonding with the $d_{x^2-y^2}$ orbital, may overlap with either the d_{xz} or d_{yz} orbital (Scheme 2) and result in the observed rhombic splitting of $g_\perp$. Azide binding at physiological pH will lead to displacement of the exchangeable ligand involved in the pH equilibrium, which allows the azide to directly donate electron density on the $d_{x^2-y^2}$ orbital, resulting in covalent delocalization of the spin density away from the copper site, leading to a decrease of β^2. The second azide binding does not change the β^2 values significantly. However, it causes a significant increase in the intensity of the $N_3^- \rightarrow Cu^{2+}$ CT band. Further, the energy of this LMCT decreases from 27000 to 23700 cm^{-1}. Although most of the ligand-field transitions in the azide-bound complexes are obscured by the $N_3^- \rightarrow Cu^{2+}$ CT transitions, a d−d band at 15503 cm^{-1} in the monoazide-bound form is shifted to lower energy to 14327 cm^{-1} in the diazide-bound form. This implies that both the N_3^- ligands interact with the $d_{x^2-y^2}$ orbital, which causes an increase of the LMCT intensity in the absorption spectrum due to direct overlap of the donor azide and acceptor $d_{x^2-y^2}$ orbital. The second ligand is a fairly covalent ligand, as indicated by the low second binding constant value of azide binding. Thus, it is likely that the $d_{x^2-y^2}$ orbital energy is lowered upon replacement of the second ligand with a weaker N_3^- ligand, which causes both the energy of the LMCT and d → d transitions to the $d_{x^2-y^2}$ orbital to be lowered.

Scheme 2. Schematic Representation of Displaceable Ligands Bound to Cu-Aβ[a]

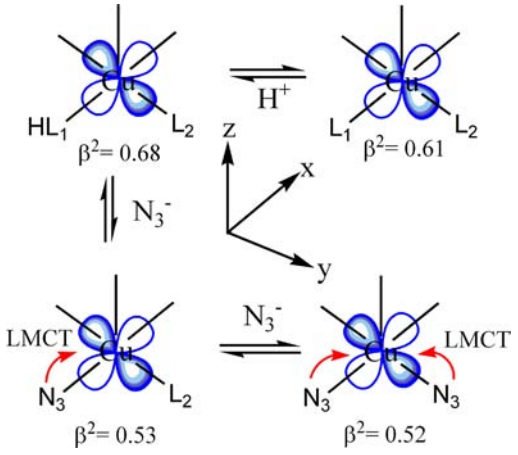

[a]The *xy* plane, which contains both exchangeable ligands, has been highlighted.

5. DISCUSSION

The EPR data of Cu^{2+}-bound native Aβ(1−16) shows the presence of component I and component II, at physiological pH.[33,62] Components I and II are in pH equilibrium with a pK_a of ~8.1. This process can either be associated with a $H_2O \leftrightarrow {}^-OH$ equilibrium or an amide C═O ↔ N^- (amidate) equilibrium. Past studies on copper-peptide complexes indicate that the pK_a value of an amide ↔ amidate equilibrium is usually in the range of 3.4−5.4.[69,72] The pK_a values of water-bound copper complexes are in the range of 7−9.[73−80] The pK_a value of 8.1 may likely suggest the equilibrium of a water-derived ligand. However, note that the local environment of the peptide around the active site can significantly tune the pK_a values because of hydrogen-bonding interactions of coordinating ligands with second-sphere residues. The presence of water as a ligand has previously been proposed by DFT and molecular dynamics studies.[46,56] These studies have also proposed an amide coordination to Cu-Aβ along with the water ligand.[56]

The ligand-field transition energies obtained from the absorption and CD data (Figure 3 and Table 3) indicate that component I of Cu-Aβ possesses high-energy ligand-field transitions (~12000−25000 cm^{-1}), suggesting a five-coordinate geometry. The axial EPR data of component I indicates a square-pyramidal geometry (a trigonal-bipyramidal geometry would reflect a d_{z^2} ground state). At high pH, all of the ligand-field transitions shift to higher energies, by about 2000 cm^{-1}. The EPR data reflect an axial ground state but with an increase in rhombicity, indicating the inequivalency of the d_{xz} and d_{yz} orbitals. The increase in the ligand field of component II and increased rhombicity are consistent with a bound hydroxide (^-OH is an anisotropic ligand), relative to a bound water in component I. The ground-state parameters obtained from the EPR data of components I and II further support a $H_2O \leftrightarrow OH$ equilibrium.[68,71] Component II with a bound hydroxide is more covalent, which accounts for a lower β^2 value and higher ligand field, relative to a water-bound component I.

The addition of 1 equiv of the clioquinol analogue, 8-hydroxyquinoline, to Cu-Aβ at pH 7 produces significant perturbation in the absorption and EPR spectra (Figures 4 and 5), implying binding of the bidentate ligand to copper. However, 1 equiv of either phenol or pyridine (binding residues of 8-hydroxyquinoline) produces little effect on the EPR data. This possibly suggests the presence of two exchangeable ligands bound to Cu-Aβ, which are replaced by the ligand because of its chelating effect. The titration of Cu-Aβ with azide at pH 7 obtained from EPR and absorption experiments (Figures 6 and

dx.doi.org/10.1021/ic301865n | *Inorg. Chem.* 2013, 52, 1318−1327

8) yields a plot with biphasic nature (Figures 8B and S7 in the Supporting Information), further supporting the presence of two exchangeable ligands. Moreover, the changes in the absorption and EPR data upon azide addition are observed at ∼100−200 equiv and another at ∼500−1000 equiv of azide addition, implying that the two replaceable ligands are of unequal strength with binding constants of 0.01 and 0.001, respectively. Thus, there exist a weak ligand and a relatively stronger ligand bound to copper, which can be replaced by 1 equiv of a chelating ligand or excess azide. Alternatively, azide binding to Cu-Aβ at high pH (component II) has no effect on the EPR and absorption data (Figures 7 B and S9 in the Supporting Information). In other words, azide cannot displace the ligand bound to copper at high pH in component II. These observations are consistent with the presence of a $^{-}$OH bound to Cu-Aβ in component II. Hydroxide, being a stronger ligand, does not get displaced by azide. Interestingly, the second exchangeable ligand also does not get displaced by azide at high pH, as reflected by the EPR data (Figures 7 B and S9 in the Supporting Information). This implies that at high pH deprotonation of one ligand, i.e., $H_2O \rightarrow {}^{-}OH$, makes the other exchangeable ligand strong as well. Note that, in contrast to azide, the bidentate 8-hydroxyquinoline ligand, binds to Cu-Aβ at high pH, likely because of its chelating effect (Figures 4B and 5B).[81] The dramatic decrease in β^2 upon displacement of the first exchangeable H_2O ligand on azide binding suggests that this ligand is in the equatorial plane and directly interacts with the $d_{x^2-y^2}$ orbital, which bears the unpaired electron. Further, the increased intensity and decreased energy of the $N_3^- \rightarrow Cu^{2+}$ CT band and decreased energy for the d−d band upon binding of the second azide suggest that the second azide also binds along the equatorial plane (Scheme 2).

The nature of the second exchangeable ligand remains ambiguous, although from ligand displacement experiments, we deduce that it is a weak exchangeable ligand at physiological pH, which becomes stronger at high pH, because it does not get displaced by azide. Coordination by amide carbonyl (C═O) would be consistent with the above observations because C═O, being a weak ligand, can be displaced by azide or 8-hydroxyquinoline. Further, the −NH adjacent to the coordinated carbonyl may directly hydrogen bond to $^{-}$OH at high pH, making C═O a stronger ligand at high pH, as observed experimentally. Several experimental reports propose the involvement of a carbonyl group of an amide as a ligand to Cu-Aβ.[41−43] NMR experiments imply the involvement of carbonyl of the peptide bond of a histidine,[42] while ENDOR and HYSCORE studies imply the carbonyl bond between Asp1 and Ala2.[41,43] Although the presence of amide has been invoked in the literature, there are no experimental reports of H_2O bound to Cu-Aβ. DFT and molecular dynamics studies propose H_2O as a fifth ligand, along with an amide coordination. Thus, the d−d transitions indicating a five-coordinate site in both components I and II and the presence of two exchangeable ligands, one of which is involved in the pH equilibrium, are most consistent with the model that reports the N terminus, C═O(Asp1−Ala2), and two histidine imidazoles (His6 and His13 or His14), along with a water molecule as the fifth ligand, as the copper binding ligands at physiological pH.[56] These results, however, do not divulge any information regarding the number and identity of the histidine ligands present.

6. CONCLUSION

In summary, copper-bound Aβ comprises components I and II under physiological conditions, which are in pH equilibrium with a pK_a value of ∼8.1. Although there are two species, Aβ peptides do not contain a second copper binding site. At high pH, component II has a higher ligand field and lower β^2 value and, hence, is bound to a more covalent ligand than the low pH counterpart, suggesting a $H_2O \leftrightarrow {}^{-}OH$ pH equilibrium. The ligand-field transitions of the two components are very high, suggesting a five-coordinate geometry in both components. Chemical perturbations of Cu-Aβ indicate the presence of two weak exchangeable ligands bound to copper along the equatorial plane, one being a H_2O ligand and the other most likely a carbonyl oxygen of the peptide bond in a square-pyramidal-type active-site geometry.

■ ASSOCIATED CONTENT

Ⓢ Supporting Information

Determination of the binding constant and EPR, optical, and absorption data. This material is available free of charge via the Internet at http://pubs.acs.org.

■ AUTHOR INFORMATION

Corresponding Author

*E-mail: icsgd@iacs.res.in.

Notes

The authors declare no competing financial interest.

■ ACKNOWLEDGMENTS

We thank the SERC Fast Track Scheme (SR/FT/CS-34/2010), Department of Science and Technology, Government of India, for funding this research. C.G. is thankful to the Council of Scientific and Industrial Research, India, for a Junior Research Fellowship. We thank Dr. Abhishek Dey for helpful discussions.

■ REFERENCES

(1) Rauk, A. *Chem. Soc. Rev.* **2009**, *38*, 2698−2715.
(2) Glenner, G. G.; Wong, C. W. *Biochem. Biophys. Res. Commun.* **1984**, *120*, 885−890.
(3) Hardy, J.; Selkoe, D. J. *Science* **2002**, *297*, 353−356.
(4) Selkoe, D. J. *Science* **2002**, *298*, 789−791.
(5) Maurer, I.; Zierz, S.; Moller, H. J. R. *Neurobiol. Aging* **2000**, *21*, 455−462.
(6) Nelson, P. G. *Curr. Alzheimer Res.* **2005**, *2*, 497−506.
(7) Seubert, P.; Vigo-Pelfrey, C.; Esch, F.; Lee, M.; Dovey, H.; Davis, D.; Sinha, S.; Schiossmacher, M.; Whaley, J.; Swindlehurst, C.; McCormack, R.; Wolfert, R.; Selkoe, D.; Lieberburg, I.; Schenk, D. *Nature* **1992**, *359*, 325−327.
(8) Whitson, J. S.; Selkoe, D. J.; Cotman, C. W. *Science* **1989**, *243*, 1488−1490.
(9) Whitson, J. S.; Glabe, C. G.; Shintani, E.; Abcar, A.; Cotman, C. W. *Neurosci. Lett.* **1990**, *110*, 319−324.
(10) Yankner, B. A.; Duffy, L. K.; Kirschner, D. A. *Science* **1990**, *250*, 279−282.
(11) Selkoe, D. J. *Nature* **1999**, *399*, A23−A31.
(12) Hou, L.; Shao, H.; Zhang, Y.; Li, H.; Menon, N. K.; Neuhaus, E. B.; Brewer, J. M.; Byeon, I.-J. L.; Ray, D. G.; Vitek, M. P.; Iwashita, T.; Makula, R. A.; Przybyla, A. B.; Zagorski, M. G. *J. Am. Chem. Soc.* **2004**, *126*, 1992−2005.
(13) Gaggelli, E.; Kozlowski, H.; Valensin, D.; Valensin, G. *Chem. Rev.* **2006**, *106*, 1995−2044.
(14) Thinakaran, G.; Koo, E. H. *J. Biol. Chem.* **2008**, *283*, 29615−29619.
(15) Kang, J.; Lemaire, H.-G.; Unterbeck, A.; Salbaum, J. M.; Masters, C. L.; Grzeschik, K.-H.; Multhaup, G.; Beyreuther, K.; Muller-Hill, B. *Nature* **1987**, *325*, 733−736.
(16) Nunan, J.; Small, D. H. *FEBS Lett.* **2000**, *483*, 6−10.

(17) Shoji, M.; Golde, T. E.; Ghiso, J.; Cheung, T. T.; Estus, S.; Shaffer, L. M.; Cai, X. D.; McKay, D. M.; Tintner, R.; Frangione, B.; Younkin, S. G. *Science* **1992**, *258*, 126−129.
(18) Vigo-Pelfrey, C.; Lee, D.; Keim, P.; Lieberburg, I.; Schenk, D. B. *J. Neurochem.* **1993**, *61*, 1965−1968.
(19) Iwatsubo, T.; Odaka, A.; Suzuki, N.; Mizusawa, H.; Nukina, N.; Ihara, Y. *Neuron* **1994**, *13*, 45−53.
(20) Smith, M. A.; Richey Harris, P. L.; Sayre, L. M.; Beckman, J. S.; Perry, G. *J. Neurosci.* **1997**, *17*, 2653−2657.
(21) Lovell, M. A.; Robertson, J. D.; Teesdale, W. J.; Campbell, J. L.; Markesbery, W. R. *J. Neurol. Sci.* **1998**, *158*, 47−52.
(22) Beauchemin, D.; Kisilevsky, R. *Anal. Chem.* **1998**, *70*, 1026−1029.
(23) Li, F.; Calingasan, N. Y.; Yu, F.; Mauck, W. M.; Toidze, M.; Almeida, C. G.; Takahashi, R. H.; Carlson, G. A.; Flint Beal, M.; Lin, M. T.; Gouras, G. K. *J. Neurochem.* **2004**, *89*, 1308−1312.
(24) Miller, L. M.; Wang, Q.; Telivala, T. P.; Smith, R. J.; Lanzirotti, A.; Miklossy, J. *J. Struct. Biol.* **2006**, *155*, 30−37.
(25) Sayre, L. M.; Perry, G.; Smith, M. A. *Curr. Opin. Chem. Biol.* **1999**, *3*, 220−225.
(26) Pramanik, D.; Dey, S. G. *J. Am. Chem. Soc.* **2011**, *133*, 81−87.
(27) Pramanik, D.; Ghosh, C.; Mukherjee, S.; Dey, S. G. *Coord. Chem. Rev.* **2013**, *257*, 81−92.
(28) Pramanik, D.; Ghosh, C.; Dey, S. G. *J. Am. Chem. Soc.* **2011**, *133*, 15545−15552.
(29) Zou, J.; Kajita, K.; Sugimoto, N. *Angew. Chem., Int. Ed.* **2001**, *40*, 2274−2277.
(30) Huang, X.; Cuajungco, M. P.; Atwood, C. S.; Hartshorn, M. A.; Tyndall, J. D. A.; Hanson, G. R.; Stokes, K. C.; Leopold, M.; Multhaup, G.; Goldstein, L. E.; Scarpa, R. C.; Saunders, A. J.; Lim, J.; Moir, R. D.; Glabe, C.; Bowden, E. F.; Masters, C. L.; Fairlie, D. P.; Tanzi, R. E.; Bush, A. I. *J. Biol. Chem.* **1999**, *274*, 37111−37116.
(31) Atwood, C. S.; Scarpa, R. C.; Huang, X.; Moir, R. D.; Jones, W. D.; Fairlie, D. P.; Tanzi, R. E.; Bush, A. I. *J. Neurochem.* **2000**, *75*, 1219−1233.
(32) Kowalik-Jankowska, T.; Ruta-Dolejsz, M.; Wisniewska, K.; Lankiewicz, L. *J. Inorg. Biochem.* **2001**, *86*, 535−545.
(33) Syme, C. D.; Nadal, R. C.; Rigby, S. E. J.; Viles, J. H. *J. Biol. Chem.* **2004**, *279*, 18169−18177.
(34) Karr, J. W.; Kaupp, L. J.; Szalai, V. A. *J. Am. Chem. Soc.* **2004**, *126*, 13534−13538.
(35) Stellato, F.; Menestrina, G.; Serra, M.; Potrich, C.; Tomazzolli, R.; Meyer-Klaucke, W.; Morante, S. *Eur. Biophys. J.* **2006**, *35*, 340−351.
(36) Minicozzi, V.; Stellato, F.; Comai, M.; Serra, M. D.; Potrich, C.; Meyer-Klaucke, W.; Morante, S. *J. Biol. Chem.* **2008**, *283*, 10784−10792.
(37) Faller, P.; Hureau, C. *Dalton Trans.* **2009**, 1080−1094.
(38) Drew, S. C.; Barnham, K. J. *Acc. Chem. Res.* **2011**, *44*, 1146−1155.
(39) Curtain, C. C.; Ali, F.; Volitakis, I.; Cherny, R. A.; Norton, R. S.; Beyreuther, K.; Barrow, C. J.; Masters, C. L.; Bush, A. I.; Barnham, K. J. *J. Biol. Chem.* **2001**, *276*, 20466−20473.
(40) Karr, J. W.; Akintoye, H.; Kaupp, L. J.; Szalai, V. A. *Biochemistry* **2005**, *44*, 5478−5487.
(41) Dorlet, P.; Gambarelli, S.; Faller, P.; Hureau, C. *Angew. Chem., Int. Ed.* **2009**, *48*, 9273−9276.
(42) Hureau, C.; Coppel, Y.; Dorlet, P.; Solari, P. L.; Sayen, S.; Guillon, E.; Sabater, L.; Faller, P. *Angew. Chem., Int. Ed.* **2009**, *48*, 9522−9525.
(43) Eury, H.; Bijani, C.; Faller, P.; Hureau, C. *Angew. Chem., Int. Ed.* **2011**, *50*, 901−905.
(44) Guilloreau, L.; Damian, L.; Coppel, Y.; Mazarguil, H.; Winterhalter, M.; Faller, P. *J. Biol. Inorg. Chem.* **2006**, *11*, 1024−1038.
(45) Karr, J. W.; Szalai, V. A. *J. Am. Chem. Soc.* **2007**, *129*, 3796−3797.
(46) Streltsov, V. A.; Titmuss, S. J.; Epa, V. C.; Barnham, K. J.; Masters, C. L.; Varghese, J. N. *Biophys. J.* **2008**, *95*, 3447−3456.
(47) Drew, S. C.; Masters, C. L.; Barnham, K. J. *J. Am. Chem. Soc.* **2009**, *131*, 8760−8761.
(48) Ali-Torres, J.; Marechal, J.-D.; Rodriguez-Santiago, L.; Sodupe, M. *J. Am. Chem. Soc.* **2011**, *133*, 15008−15014.
(49) Miura, T.; Suzuki, K.; Kohata, N.; Takeuchi, H. *Biochemistry* **2000**, *39*, 7024−7031.
(50) Kowalik-Jankowska, T.; Ruta, M.; Wisniewska, K.; Lankiewicz, L. *J. Inorg. Biochem.* **2003**, *95*, 270−282.
(51) Drew, S. C.; Noble, C. J.; Masters, C. L.; Hanson, G. R.; Barnham, K. J. *J. Am. Chem. Soc.* **2009**, *131*, 1195−1207.
(52) Curtain, C. C.; Ali, F. E.; Smith, D. G.; Bush, A. I.; Masters, C. L.; Barnham, K. J. *J. Biol. Chem.* **2003**, *278*, 2977−2982.
(53) Sarell, C. J.; Syme, C. D.; Rigby, S. E. J.; Viles, J. H. *Biochemistry* **2009**, *48*, 4388−4402.
(54) Alies, B.; Eury, H. l. n.; Bijani, C.; Rechignat, L.; Faller, P.; Hureau, C. *Inorg. Chem.* **2011**, *50*, 11192−11201.
(55) Shin, B.-k.; Saxena, S. *Biochemistry* **2008**, *47*, 9117−9123.
(56) Furlan, S.; Hureau, C.; Faller, P.; La Penna, G. *J. Phys. Chem. B* **2012**, *116*, 11899−11910.
(57) Ginotra, Y. P.; Ramteke, S. N.; Srikanth, R.; Kulkarni, P. P. *Inorg. Chem.* **2012**, *51*, 7960−7962.
(58) Reem, R. C.; Solomon, E. I. *J. Am. Chem. Soc.* **1987**, *109*, 1216−1226.
(59) Cole, J. L.; Clark, P. A.; Solomon, E. I. *J. Am. Chem. Soc.* **1990**, *112*, 9534−9548.
(60) Pulver, S.; Froland, W. A.; Fox, B. G.; Lipscomb, J. D.; Solomon, E. I. *J. Am. Chem. Soc.* **1993**, *115*, 12409−12422.
(61) Yoon, J.; Liboiron, B. D.; Sarangi, R.; Hodgson, K. O.; Hedman, B.; Solomon, E. I. *Proc. Natl. Acad. Sci. U.S.A.* **2007**, *104*, 13609−13614.
(62) Shin, B.-k.; Saxena, S. *J. Phys. Chem. A* **2011**, *115*, 9590−9602.
(63) Garzon-Rodriguez, W.; Yatsimirsky, A. K.; Glabe, C. G. *Bioorg. Med. Chem. Lett.* **1999**, *9*, 2243−2248.
(64) Jiang, D.; Men, L.; Wang, J.; Zhang, Y.; Chickenyen, S.; Wang, Y.; Zhou, F. *Biochemistry* **2007**, *46*, 9270−9282.
(65) Bush, A. I.; Tanzi, R. E. *Neurotherapeutics* **2008**, *5*, 421−432.
(66) Cole, J. L.; Avigliano, L.; Morpurgo, L.; Solomon, E. I. *J. Am. Chem. Soc.* **1991**, *113*, 9080−9089.
(67) Zink, J. I.; Drago, R. S. *J. Am. Chem. Soc.* **1972**, *94*, 4550−4554.
(68) Chen, P.; Solomon, E. I. *J. Am. Chem. Soc.* **2004**, *126*, 4991−5000.
(69) Hamburg, A. W.; Nemeth, M. T.; Margerum, D. W. *Inorg. Chem.* **1983**, *22*, 3535−3541.
(70) Quintanar, L.; Yoon, J.; Aznar, C. P.; Palmer, A. E.; Andersson, K. K.; Britt, R. D.; Solomon, E. I. *J. Am. Chem. Soc.* **2005**, *127*, 13832−13845.
(71) Basumallick, L.; Sarangi, R.; DeBeer George, S.; Elmore, B.; Hooper, A. B.; Hedman, B.; Hodgson, K. O.; Solomon, E. I. *J. Am. Chem. Soc.* **2005**, *127*, 3531−3544.
(72) Dennis, C. R.; Swarts, J.; Margerum, D. *React. Kinet., Mech. Catal.* **2012**, *107*, 27−38.
(73) Bertini, I.; Canti, G.; Luchinat, C.; Scozzafava, A. *J. Chem. Soc., Dalton Trans.* **1978**, 1269−1273.
(74) Young, M. J.; Wahnon, D.; Hynes, R. C.; Chin, J. *J. Am. Chem. Soc.* **1995**, *117*, 9441−9447.
(75) Lanznaster, M.; Neves, A.; Bortoluzzi, A.; Aires, V. E.; Szpoganicz, B.; Terenzi, H. N.; Severino, P.; Fuller, J.; Drew, S.; Gahan, L.; Hanson, G.; Riley, M.; Schenk, G. *J. Biol. Inorg. Chem.* **2005**, *10*, 319−332.
(76) Wall, M.; Linkletter, B.; Williams, D.; Hynes, R. C.; Chin, J. *J. Am. Chem. Soc.* **1999**, *121*, 4710−4711.
(77) Okajima, T.; Kishishita, S. I.; Chiu, Y.-C.; Murakawa, T.; Kim, M.; Yamaguchi, H.; Hirota, S.; Kuroda, S. I.; Tanizawa, K. *Biochemistry* **2005**, *44*, 12041−12048.
(78) Groves, J. T.; Rife, R.; Chambers, R. *J. Am. Chem. Soc.* **1984**, *106*, 630−638.
(79) Berreau, L. M. Water Activation: Catalytic Hydrolysis. *Activation of Small Molecules*; Wiley-VCH Verlag GmbH & Co. KGaA: Weinheim, Germany, 2006; pp 287−317.
(80) Rokhsana, D.; Shepard, E. M.; Brown, D. E.; Dooley, D. M. Amine Oxidase and Galactose Oxidase. *Copper−Oxygen Chemistry*; John Wiley & Sons, Inc.: New York, 2011; pp 53−106.
(81) Changes in the absorption data of 8-hydroxyquinoline-bound Cu-Aβ at high and low pH may be due to changes in hydrogen-bonding interactions with the ligand.